IFSCC 2025 full paper (IFSCC2025-1195)

# Comprehensive analysis of the protective effects of carnosine and resveratrol combination on skin photodamage using HFF cells and 3D dermal skin model

**Minhua Hong * [1] , Xianglong Zhao [1] , Jin Liu [1] , Diqing Wang [1] , Hui Wang [1]and Rong Tang [1]**
[1]Shanghai Peptide Biotechnology Co.,Ltd, Shanghai, China

## 1. Introduction

Ultraviolet (UV) radiation is ubiquitous and poses a significant threat to skin health[1].Prolonged exposure to UV can cause acute photodamage, such as sunburn and erythema, and chronic photoaging, characterized by wrinkles, sagging, and hyperpigmentation[2]. Moreover, UV radiation is a major inducer of photocarcinogenesis. Therefore, developing effective UV protection strategies is of great scientific and clinical significance.

In the field of skin photoprotection, natural bioactive compounds have garnered attention due to their safety and potential for multitarget effects. Carnosine, an endogenous dipeptide (β-alanyl-L-histidine), is widely found in mammalian tissues and exhibits multiple biological functions[3]. Its antioxidant properties include direct scavenging of reactive oxygen species (ROS) such as hydroxyl radicals and hydrogen peroxide, as well as chelation of transition metal ions (e.g., $Fe^{2+}$ and $Cu^{2+}$) to inhibit lipid peroxidation[4]. Carnosine also possesses anti-glycation characteristics, reducing the formation of advanced glycation end products (AGEs) and preventing AGE-induced collagen cross-linking and hardening. Additionally, its anti-inflammatory effects are mediated through the inhibition of the NF-κB pathway, downregulating the expression of pro-inflammatory factors such as interleukin-6 (IL-6) and tumor necrosis factor-α (TNF-α) [5]. Preclinical studies have shown that carnosine can improve UVB-induced erythema in mice and promote fibroblast proliferation[6]. However, the efficacy of a single component is limited in the complex UV damage mechanism.

Resveratrol, a natural polyphenolic compound found in grapes and Polygonum cuspidatum, has been widely proven to have photoprotective effects. It activates the silent information regulator 1 (SIRT1) and nuclear factor erythroid 2-related factor 2 (Nrf2) pathways, enhancing the expression of antioxidant enzymes such as superoxide dismutase (SOD) and glutathione peroxidase (GPx), thereby increasing cellular resistance to oxidative stress[7]. Resveratrol also inhibits the transcription of matrix metalloproteinases (MMPs) such as MMP-1 and MMP-3, reducing collagen degradation and blocking UV-induced MAPK/ERK signaling pathways to alleviate inflammatory responses[8]. Furthermore, it promotes the expression of DNA damage repair proteins (e.g., XPC and XRCC1), directly intervening in UVB-induced DNA damage[9].

It is noteworthy that UV-induced skin damage involves multiple interrelated pathological processes, including oxidative stress, inflammatory responses, collagen metabolism imbalance, and cell apoptosis. A single component is unlikely to comprehensively intervene in these processes. For example, carnosine efficiently scavenges ROS but has weak inhibitory effects on MMPs. Resveratrol regulates the Nrf2 and SIRT1 pathways but has limited intervention in glycation damage[10]. The combination of these two components may produce synergistic effects through multitarget mechanisms of "antioxidation, anti-inflammation, and collagen protection."

For instance, carnosine reduces ROS generation to alleviate the metabolic burden on resveratrol, while resveratrol activates the Nrf2 pathway to enhance carnosine's antioxidant capacity. Together, they inhibit NF-κB-mediated inflammatory cascades, thereby more effectively combating UV damage[11]. However, current research on the combination of carnosine and resveratrol is mainly focused on anti-aging and diabetic complications, and the synergistic protective mechanisms and optimal ratios for skin photodamage remain unclear, which is a key issue limiting their practical application.

This study addresses the above scientific questions by first using human fibroblasts (HFF) to screen for the safe concentrations and optimal combination ratios of carnosine and resveratrol. Antioxidant indicators and gene expression analyses were used to determine the most suitable concentrations and ratios of the combination. Subsequently, a 3D dermal skin model induced by UVA was constructed to simulate the real skin microenvironment. Histological staining (HE) and immunofluorescence (IF) were employed to evaluate the repair effects of the combination on the dermal structure (cell density and collagen fiber arrangement). This study fills the research gap in the field of skin photoprotection using the "carnosine-resveratrol" combination, providing a theoretical basis for the development of new photoprotective formulations with antioxidant, anti-inflammatory, and collagen-protective functions.

## 2. Methods

2.1 Cell Viability Assay:

(1) Fibroblasts were used in this study. When the cell density reached 80-100%, the old medium was discarded and the cells were washed with PBS. 2 ml of 0.25% trypsin was added and incubated at 37°C for 5 minutes. The cells were then resuspended in the culture medium after centrifugation (1000 rpm, 3 minutes). The cell suspension was counted on a cell counting slide, and $1\times10^4$ cells per well were seeded in a 96-well plate. The plate was then incubated in a $CO_2$ incubator at 37°C and 5% $CO_2$ for 24 hours. Specific information is shown in Table 1.

(2) After cell treatment, 20 μl of CCK-8 solution was added to each well, and the plate was further incubated in the incubator for 1 hour. The absorbance was measured at 450 nm using a microplate reader to calculate cell viability.

2.2 Detection of SOD Activity and MDA Levels in Fibroblasts:

Cells were seeded at a density of $2\times10^5$ cells per well in a 6-well plate and cultured for 24 hours. Different groups of samples were treated for 24 hours, followed by 4 hours of $H_2O_2$ treatment. The cells were washed twice with PBS, and lysed with cell lysis buffer to collect the cell lysates. The contents of SOD and MDA in the cell supernatant were detected according to the kit instructions.

2.3 Quantitative Gene Detection (QGP):

(1) Experimental groups (Carnosine, Resveratrol) and a negative control group without drug treatment were established. Cells were seeded at a density of $6\times10^4$ cells per well in a 24-well plate with a volume of 0.5 ml per well. The plate was cultured in the incubator for 24 hours. After culture, the supernatant was discarded, and 0.2 ml of cell lysis buffer (Lysis Mixture) was added to lyse the cells. The lysed cells were stored at -80°C.

(2) The Working Bead Mix was prepared according to the instructions and 20 μL was added to each well of the Hybridization Plate. Simultaneously, 80 μL of Cell Lysates and Diluted Lysis Mixture were added. The Hybridization Plate was sealed and incubated at 54±1°C, 600 rpm for 18-22 hours.

(3) The Pre-Amplifier Solution, Amplifier Solution, and Label Probe Solution were brought to room temperature and then incubated at 37°C for 30 minutes.

(4) The Hybridization Plate was centrifuged, the seal was removed, and the solution was mixed by pipetting up and down five times. The solution was then transferred to the Magnetic Separation Plate. The plate was washed by placing it in a washing machine, and the solution was removed by inverting the plate. The reaction was carried out. After incubation, the plate was washed, and the washing steps were repeated. SAPE was bound, and the SAPE reaction was carried out. The plate was washed again, and the washing steps were repeated. 130 μL of SAPE Wash Buffer was added to each well, mixed by shaking, and the detection analysis was performed.

2.4 Preparation of the 3D Dermal Skin Model:

(1) Collagen neutralization solution was prepared. On ice, collagen type I solution was mixed with 10× DMEM medium at a ratio of 8:1, and the pH of the collagen mixture was adjusted to 7.2-7.6 with 1M NaOH. The mixture was then mixed evenly and kept on ice for later use.

(2) The collagen neutralization solution was mixed with an equal volume of cell suspension at a cell density of $0.5\times10^6$/mL.

(3) The collagen-cell mixture was added to the center of a 24-well plate (in a circular shape without touching the inner wall). The plate was then transferred to a $CO_2$ incubator at 37°C and 5% $CO_2$ for 1 hour to allow polymerization. After polymerization, an appropriate amount of complete medium was added.

(4) The cultured dermal skin model was imaged every other day using a high-content imaging system to observe cell growth and model morphological changes for subsequent experimental use.

2.5 HE Staining:

(1) Fixation: The 3D skin model after UVA irradiation was carefully removed from the culture dish and placed in 4% paraformaldehyde solution for fixation at room temperature for 24-48 hours (without shaking). The paraformaldehyde was discarded, and the samples were immersed in PBS for 2 hours, followed by gradient dehydration. Paraffin embedding: The samples were immersed in two paraffin baths for 1 hour each. The embedded skin model was placed in an embedding box, filled with liquid paraffin at 60°C, and the paraffin block was then placed on a cooling stage for 12 hours. The paraffin block was removed after cooling. The paraffin-embedded samples were sectioned using a microtome. The paraffin sections were dewaxed and dehydrated, and finally immersed in PBS, which was agitated for 5 minutes three times. The sections were then placed in hematoxylin staining solution for 5 minutes, followed by rinsing with tap water to remove excess stain.

(2) The sections were placed in hydrochloric acid ethanol for differentiation for 2-3 seconds, rinsed with tap water, and then blued for 5 minutes. The sections were then placed in eosin staining solution for 5 seconds. After drying the sections in a 37°C oven, they were immersed in xylene for 5 minutes. The sections were then placed in a ventilated area to allow the xylene to evaporate, and the sections were sealed with neutral resin. The sections were finally observed under a microscope.

2.6 Immunofluorescence:

(1) The 3D skin model after UVA irradiation was carefully removed from the culture scaffold to avoid mechanical damage and immersed in 4% paraformaldehyde solution for fixation at room temperature for 2 hours. After fixation, the samples were washed three times with PBS (5 minutes each) to remove residual fixative. The samples were then transferred to a 0.3% Triton X-100 solution and incubated at room temperature for 1 hour. The samples were blocked with 5% BSA (or 10% normal goat serum) at room temperature for 1 hour. Primary antibody incubation: According to the antibody instructions, the primary antibody was diluted to the working concentration (e.g., anti-COL1A1 antibody at 1:200). The samples were immersed in the primary antibody solution and incubated at 4°C overnight. Negative controls (omitting the primary

antibody) and positive controls (tissues known to express the target protein) were set up. Secondary antibody incubation: The samples were washed three times with PBS (5 minutes each) to remove unbound primary antibody. Fluorescent-labeled secondary antibody (e.g., Alexa Fluor 488 goat anti-rabbit IgG, diluted 1:500) was added and incubated at room temperature in the dark for 1 hour.

(2) After washing with PBS, the samples were immersed in DAPI solution (1:1000 dilution) and incubated at room temperature in the dark for 5 minutes. The samples were mounted on slides with an antifade mounting medium (SlowFade Gold), covered with a coverslip to avoid bubbles, and allowed to dry in the dark for 24 hours. The samples were then stored at 4°C. Images were captured and stored using a confocal laser scanning microscope. ImageJ software was used for image analysis.

2.7 Statistical Analysis:

GraphPad Prism was used for data plotting, with results expressed as Mean±SD. Comparisons between groups were analyzed using t-tests. A p-value of less than 0.05 was considered statistically significant, and a p-value of less than 0.01 was considered highly significant.

## 3. Results

The present study systematically evaluated the protective effects of the combination of carnosine and resveratrol on UV-induced skin photodamage using fibroblasts and a 3D dermal skin model.

3.1 The Optimal Combination Ratio of Carnosine and Resveratrol is 3:1

The viability of fibroblasts treated with carnosine and resveratrol individually and in combination is shown in Figure 1. The combination ratios of carnosine and resveratrol were 1:3, 1:1, and 3:1. The results indicated that the combination ratios of 1:3 and 1:1 significantly reduced fibroblast viability (cell viability below 80%). When the combination ratio was 3:1, no significant effect on fibroblast viability was observed. Therefore, this ratio was considered the optimal combination ratio. This study provides valuable reference for determining the combination ratio and safe concentration of peptides and bioactive compounds.

3.2 Significant Antioxidant Capacity of the Resveratrol and Carnosine Combination

As shown in Figures 2a and 2b, compared with the PC group, the combination of carnosine and resveratrol significantly increased the activity of superoxide dismutase (SOD) in cells by 51.48% and reduced the content of malondialdehyde (MDA) by 42.3%. These results demonstrate that the combination of carnosine and resveratrol has significant antioxidant capacity and can effectively protect fibroblasts from oxidative stress damage.

3.3 Significant Enhancement of Collagen Synthesis by the Carnosine and Resveratrol Combination

As shown in Figure 3, after treatment with the combination of carnosine and resveratrol, fibroblasts significantly upregulated the expression of antioxidant defense genes *NFE2L2* and *SOD2*, as well as collagen synthesis genes *COL3A1* and *COL1A1*, while significantly downregulating the expression of aging-related gene *MMP1* and inflammation-related gene *IL-6*. These results indicate that the combination of carnosine and resveratrol can significantly enhance the collagen synthesis capacity and antioxidant capacity of dermal cells, effectively inhibiting skin inflammation and aging.

3.4 Significant Repair Effects of the Carnosine and Resveratrol Combination on Photodamaged Dermis

As shown in Figure 4a, UVA irradiation leads to degradation and disorganization of collagen fibers in the dermis, as well as a decrease in fibroblast number, manifested as sparse and broken collagen fibers and reduced cell density in HE staining. As shown in Figure 4b, after treatment with the carnosine and resveratrol combination, the cell density in the dermis increased and collagen fibers were more densely arranged, confirming the significant repair effects of the combination on photodamaged dermis.

3.5 Significant Increase in Col1A1 Expression in the Dermis by the Carnosine and Resveratrol Combination

As shown in Figures 5a and 5b, after UVA irradiation, the expression of type I collagen (Col1A1) in the 3D dermal skin model treated with the carnosine and resveratrol combination significantly increased, with increased cell number and regular arrangement in the dermis. These results indicate that the combination of carnosine and resveratrol can significantly enhance collagen synthesis capacity, reduce tissue damage, and provide significant protection for the skin.

**Table 1.** Experimental Design

| No. | Group Name | Final Concentration (mg/ml) |
|---|---|---|
| Negative Control | Untreated complete medium containing cells | - |
| Single set of samples | Carnosine | 0.02 |
| | Resveratrol | 0.2 |
| | Carnosine + Resveratrol | 3:1、2:2、1:3 |

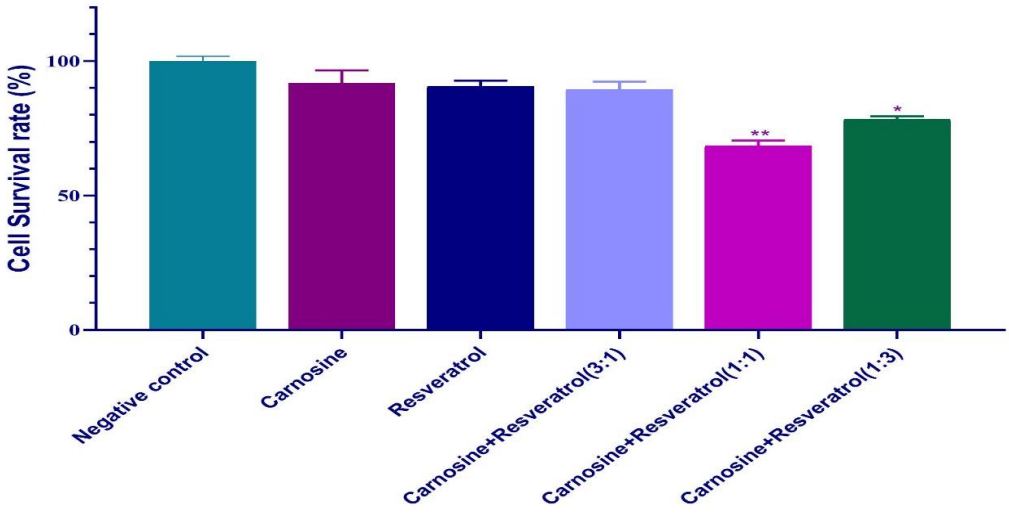


**Figure 1.** Cytotoxicity of different ratios of carnosine and resveratrol combination.
Negative control: Cell viability of cells without any drug treatment; Error bars represent the standard deviation of three replicates; *: p-value < 0.05, **: p-value < 0.01.

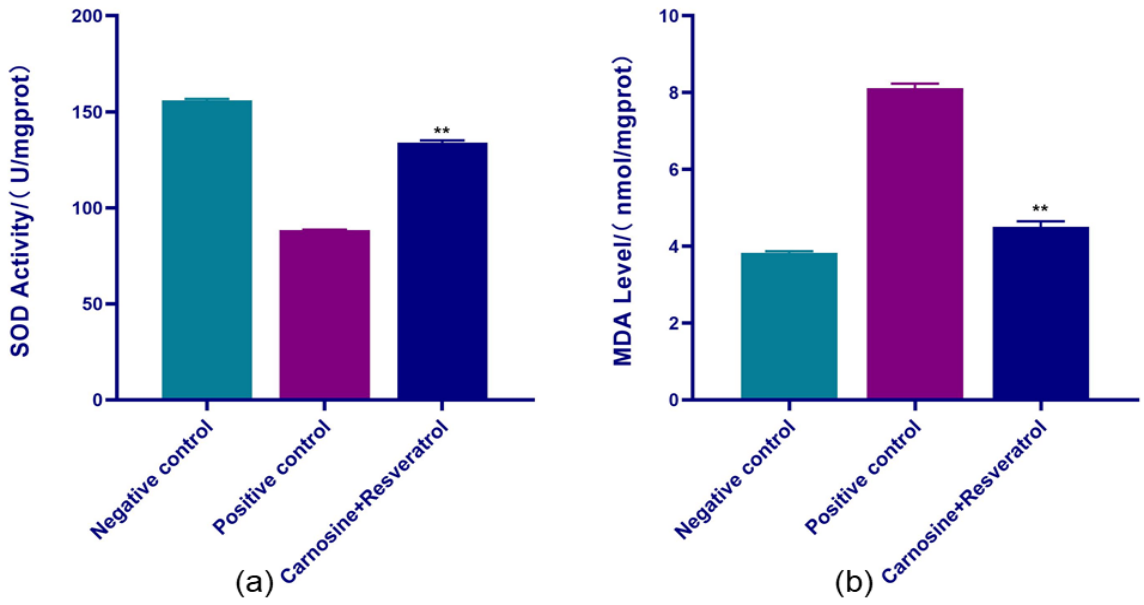


**Figure 2.** Detection of antioxidant indicators in fibroblasts.
(a) SOD activity in fibroblasts. (b) Changes in MDA concentration.Negative control (NC): MDA concentration and SOD activity measured in cells without any drug treatment; Positive control (PC): MDA levels and SOD activity measured in cells treated with 500 μM $H_2O_2$. Error bars represent the standard deviation of three replicates; *: p-value < 0.05, **: p-value < 0.01.

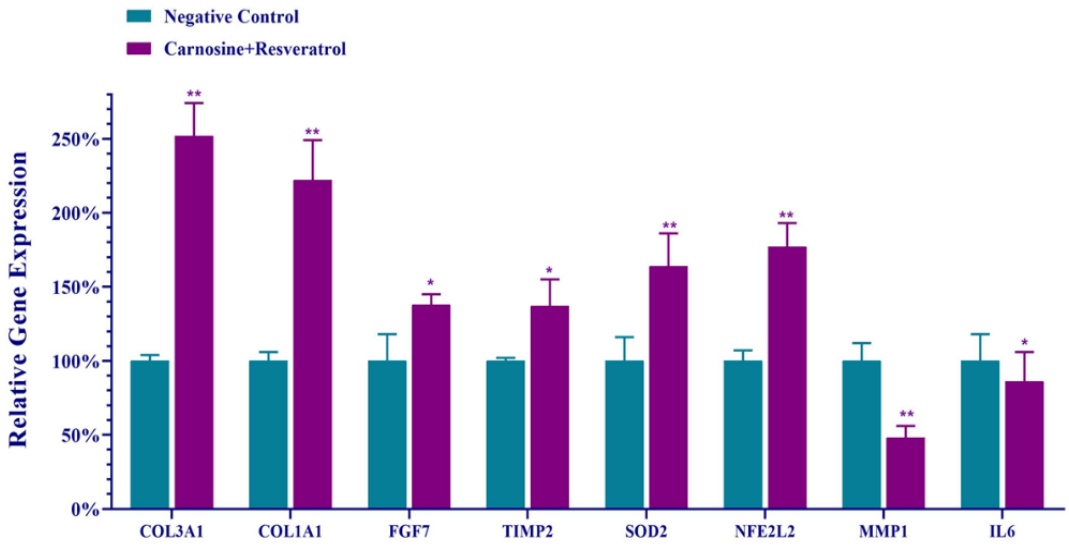


**Figure 3.**Changes in gene expression after treatment with carnosine and resveratrol.
Error bars represent the standard deviation of three replicates; *: p-value < 0.05, **: p-value < 0.01.

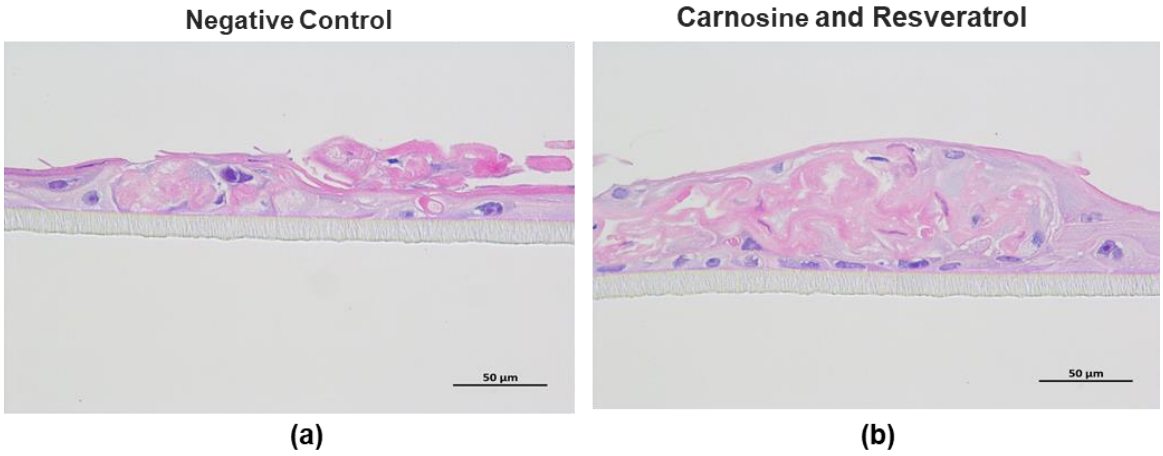


**Figure 4.**HE (Hematoxylin and Eosin) staining of the 3D dermal skin model.
(a) HE staining of the skin model after UVA irradiation without any treatment. (b) HE staining of the skin model after UVA irradiation treated with the carnosine and resveratrol combination. Scale bar: 500 µm, Blue: Nuclei; Red: Cytoplasm.

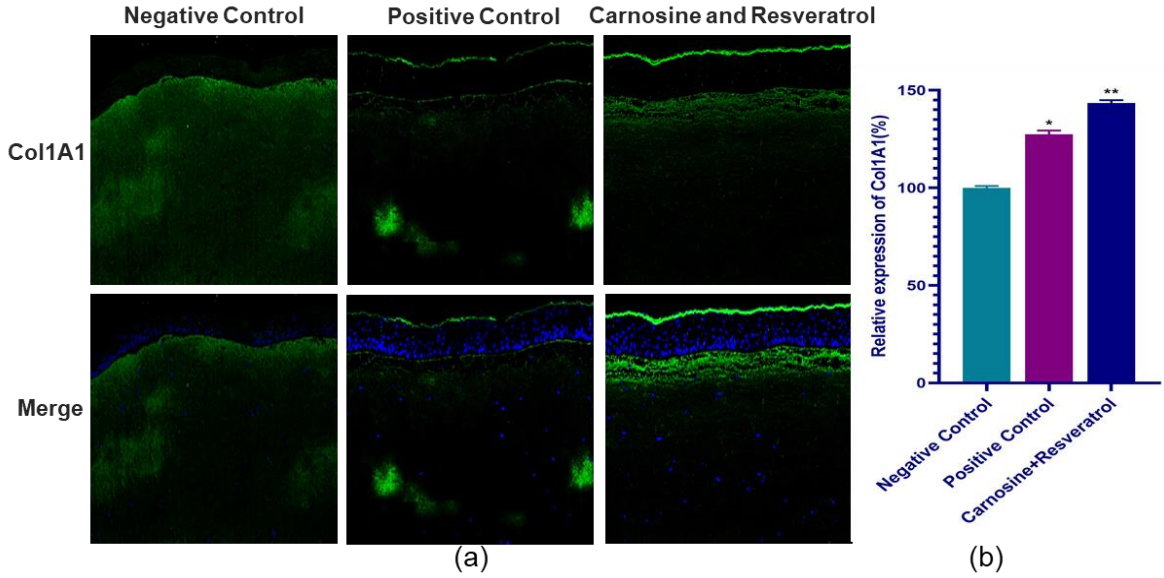


**Figure 5**.Immunofluorescence staining of the 3D dermal skin model (IF).
(a) Localization and expression of type I collagen (Col1A1). (b) Statistical analysis of the average expression of Col1A1; Negative control: Skin model after UVA irradiation without any drug treatment, Positive control: Skin model treated with TGF and UVA irradiation, Skin model treated with the carnosine and resveratrol combination and UVA irradiation. Error bars represent the standard deviation of three replicates; *: p-value < 0.05, **: p-value < 0.01.

## 4. Discussion

This study systematically verified the protective effects of the carnosine and resveratrol combination on UV-induced skin photodamage using human fibroblasts (HFF) and a 3D dermal skin model. From the perspective of antioxidant mechanisms, the combination was confirmed to scavenge free radicals and inhibit lipid peroxidation by reducing MDA levels and increasing SOD activity[12].Compared with existing studies, this study innovatively combined in vitro cell

models with 3D skin models that are closer to the physiological environment, discovering the repair effects of the combination on dermal structure in a simulated real skin microenvironment. Previous studies on carnosine and resveratrol have mostly focused on individual components or non-photodamage scenarios (e.g., antiglycation or anti-aging), while this study first confirmed their synergistic effects in a UV damage model, especially by regulating key genes such as COL1A1 and NFE2L2, revealing a triple protection mechanism of "antioxidation-anti-inflammation-collagen protection[13]." However, the study still has certain limitations: for example, the transdermal absorption efficiency and pharmacokinetics of the combination in vivo have not been clarified; moreover, the long-term effects of the combination on photocarcinogenesis need further investigation[14]. Future research can be expanded to multi-wavelength UV damage models, combined with animal experiments to verify in vivo efficacy, and explore nanocarrier technologies to enhance the bioavailability of the components, providing a more solid foundation for clinical application.

## 5. Conclusion

This study clarified that the optimal combination ratio of carnosine and resveratrol is 3:1 using fibroblasts and a 3D dermal skin model. The combination can effectively alleviate UV-induced oxidative damage and inflammatory responses by significantly reducing MDA levels, enhancing *SOD* activity, and regulating the expression of key genes such as *NFE2L2, MMP1, IL-6*, and *COL1A1*. In the 3D skin model, the combination further confirmed its protective effects on type I collagen in the dermis and its capacity for damage repair. This study provides multidimensional experimental evidence for the protection of skin photodamage. The synergistic effects of the combination were revealed for the first time, especially in regulating key gene expression and improving skin structure. The enhanced effects of the combination may originate from the complementary abilities of carnosine's antiglycation and resveratrol's free radical scavenging, thereby more comprehensively resisting the multiple damages caused by UV radiation. The combination can be used as a potential effective component for the development of functional skincare products or drugs for anti-photoaging and photodamage repair, providing important theoretical basis and scientific support for formula development in related fields.

[1]Moshammer H, Simic S, Haluza D. UV-Radiation: From Physics to Impacts. *Int J Environ Res Public Health*. 2017;14(2):200. Published 2017 Feb 17.

[2]Bauwens E, Parée T, Meurant S, et al. Senescence Induced by UVB in Keratinocytes Impairs Amino Acids Balance. *J Invest Dermatol*. 2023;143(4):554-565.e9.

[3]Artioli GG, Sale C, Jones RL. Carnosine in health and disease. *Eur J Sport Sci*. 2019;19(1):30-39.

[4]Hipkiss AR, Baye E, de Courten B. Carnosine and the processes of ageing. *Maturitas*. 2016;93:28-33.

[5]Banerjee S, Mukherjee B, Poddar MK, Dunbar GL. Carnosine improves aging-induced cognitive impairment and brain regional neurodegeneration in relation to the neuropathological alterations in the secondary structure of amyloid beta (Aβ). *J Neurochem*. 2021;158(3):710-723.

[6] Owjfard M, Rahimian Z, Karimi F, Borhani-Haghighi A, Mallahzadeh A. A comprehensive review on the neuroprotective potential of resveratrol in ischemic stroke. *Heliyon*.2024;10(14):e34121. Published 2024 Jul 5.

[7] Huang WC, Liou CJ, Shen SC, et al. Punicalagin from pomegranate ameliorates TNF-α/IFN-γ-induced inflammatory responses in HaCaT cells via regulation of SIRT1/STAT3 axis and Nrf2/HO-1 signaling pathway. *Int Immunopharmacol*. 2024;130:111665.

[8] Liu H, Zhu S, Han W, Cai Y, Liu C. DMEP induces mitochondrial damage regulated by

inhibiting Nrf2 and SIRT1/PGC-1α signaling pathways in HepG2 cells. *Ecotoxicol Environ Saf*. 2021;221:112449.
[9] Pittayapruek P, Meephansan J, Prapapan O, Komine M, Ohtsuki M. Role of Matrix Metalloproteinases in Photoaging and Photocarcinogenesis. *Int J Mol Sci*. 2016;17(6):868. Published 2016 Jun 2.
[10] Cui B, Wang Y, Jin J, et al. Resveratrol Treats UVB-Induced Photoaging by Anti-MMP Expression, through Anti-Inflammatory, Antioxidant, and Antiapoptotic Properties, and Treats Photoaging by Upregulating VEGF-B Expression. *Oxid Med Cell Longev*. 2022;2022:6037303. Published 2022 Jan 4.
[11] Mavragani IV, Nikitaki Z, Souli MP, et al. Complex DNA Damage: A Route to Radiation-Induced Genomic Instability and Carcinogenesis. *Cancers (Basel)*. 2017;9(7):91. Published 2017 Jul 18.
[12] Selvaraj V, Sekaran S, Dhanasekaran A, Warrier S. Type 1 collagen: Synthesis, structure and key functions in bone mineralization. *Differentiation*. 2024;136:100757.
[13] Sanada A, Yamada T, Hasegawa S, et al. Enhanced Type I Collagen Synthesis in Fibroblasts by Dermal Stem/Progenitor Cell-Derived Exosomes. *Biol Pharm Bull*. 2022;45(7):872-880.
[14] Gao Y, Ma K, Kang Y, et al. Type I collagen reduces lipid accumulation during adipogenesis of preadipocytes 3T3-L1 via the YAP-mTOR-autophagy axis. *Biochim Biophys Acta Mol Cell Biol Lipids*. 2022;1867(9):159181.